



CERT

**Comité d'évaluation des
ressources transfrontalières**

Document de travail 2014/16

Ne pas citer sans
autorisation des auteurs

TRAC

**Transboundary Resources
Assessment Committee**

Working Paper 2014/16

Not to be cited without
permission of the authors

Gear avoidance behavior of yellowtail flounder associated with the HabCam towed imaging vehicle.

Burton Shank and Jon Duquette

NOAA /NMFS/ NEFSC
Population Dynamics Branch
Woods Hole, Ma



ABSTRACT

Estimating the efficiency of survey gear is difficult in the absence of having known densities of target organisms. Image based surveys have the advantage of both providing an abundance estimate and recording the behavior of the organism and its reaction to the gear at the time it was sampled (Uzmann 1977). We explored how this recorded behavior may be informative for understanding the catchability of the imaging gear itself, using an image library from the HabCam towed underwater vehicle. Yellowtail flounder exhibited clear diel behavioral patterns. While most individuals were recorded resting on the substrate, 30% of individuals observed at night were partially buried in the sediment and 30% of the individuals observed during the daytime were swimming near the bottom, most of which were confirmed to be fleeing the vehicle. There were no strong patterns in the directional orientation of flounder resting on the bottom but most of the flounder reacting to the vehicle were swimming towards the vehicle rather than away from it. Most swimming fish were observed in the same image where they had been resting or in the adjacent image but some fish covered longer distances, suggesting that a fish that swam perpendicular to the image track could escape being photographed. We conclude that burying behavior or gear avoidance could marginally decrease the catchability of yellowtail in HabCam imagery. The observed diel patterns in burying behavior and gear avoidance may also provide insight into diel variations in efficiency observed for other mobile gear types.

Introduction

HabCam is an underwater imaging vehicle that is towed approximately 2 meters above the bottom and captures overlapping digital still images. The vehicle has been used extensively for surveying the sea scallop resource on Georges Bank and the Mid Atlantic Bight as well as collecting data on finfish and habitat. In addition to capturing the presence and size of animals, it also captures behavior, including avoidance of the vehicle itself. In many cases, the capture efficiency of imaging systems is assumed to be near 100%, making them good candidates for estimating the efficiency of other fishing gear like dredges and bottom trawls (Somerton et al. 1999, Lauth et al. 2004a). However, the efficiency of imaging systems may decrease as the mobility of organism increase, allowing them to avoid the sampling gear or as they become increasingly cryptic (Gunderson 1993, Adams et al. 1995, Trenkel et al. 2004). Here, we examine an image library of yellowtail flounder (*Limanda ferruginea*) from a HabCam survey in 2010 to document their behavior in response to the sampling vehicle. We recorded their behavior, orientation relative to the vehicle, and flight distance to determine how cryptic behavior and gear avoidance may impact the efficiency of abundance data collected by this gear.

Methods

Our study used the data from the HabCam group RSA survey of Closed Area 2 South, conducted from Aug 1-4, 2010 (Figure 1). From this survey, data were available from 182,006 images, including 273 observations of yellowtail flounder. Because the substrate in the study region is mostly sandy bottom, flatfish, resting on the bottom and startled by the vehicle typically flush clouds of sediment into the water that are apparent in the images.

Behavior data was extracted from the images using a web-interface image annotator developed by collaborators at the Woods Hole Oceanographic Institute. The annotator allows the user to record data to a PostgreSQL database that also houses the image metadata including image location, date and time, vehicle altitude, and field of view.

To document the behavioral state of yellowtail, we examined the 273 images and categorized their behavior as resting on the surface, swimming, or buried (some portion of the dorsal or anal fin covered with sediment). When necessary, we checked the adjacent, overlapping images to confirm that “swimming” fish were off the bottom and moving. When fish were confirmed as swimming, we examined the twelve images immediately before and after the image with the fish for evidence of a sediment cloud, indicating that the fish had been resting on the bottom and had responded to the vehicle by attempting to avoid it (see Laugh et al. 2004b). When sediment clouds were evident, the behavior of the fish was re-classified as fleeing. For all fish observed in images, we marked a line segment from the tip of the rostrum to the center of the caudal peduncle to record the orientation of the fish relative to the vehicle.

For the fish classified as fleeing, we calculated the distance that they swam between the sediment cloud where they had been resting and the fish’s location in the image where they were recorded. As the fish and the sediment cloud were commonly on different images, we measured the distance across the images by marking line segments between stationary reference points, typically pieces of shell hash, that were visible in adjacent images (Figure 2). The total distance traveled by a fish during flight was calculated as:

$$X_{\text{disp}} = \sum_{i=1, k} (x_{i2} - x_{i1}) * \text{MmPix} / 1000$$

$$Y_{\text{disp}} = \sum_{i=1, k} (y_{i2} - y_{i1}) * \text{MmPix} / 1000$$

Where X_{disp} and Y_{disp} are the net displacement in meters across and along the survey track between the sediment cloud, (x_{i1}, y_{i1}) and (x_{i2}, y_{i2}) are the coordinates of the reference points in image i , k is the number of images between the sediment cloud and the fish and MmPix is the number of millimeters per pixel, calculated based on the vehicle altitude, roll, and pitch.

Results

The observed behavior of yellowtail varied on a diel basis. Fish were most commonly seen resting on the surface (68% Table 1, Figure 3). 30% of fish observed at night and 8% of all fish observed were partially buried (Figure 4). Similarly, 30% of fish observed in the day and 23% of all fish observed were swimming. Of the 64 fish observed to be actively swimming, 59 of them (92%) could be traced back to a sediment cloud and were re-classified as “fleeing”. Swimming or fleeing fish were observed only during daylight hours. Conversely, of the 22 fish that were observed to be partially buried, all but one were observed during the nighttime. The one daytime observation of burying was at 19:54 with sunset at approximately 20:45.

Fish density was higher in the west central portion of the study area (Figure 5, 6). Space (Longitude) and time of day were correlated in the survey layout, with pre-dawn sampling consistently occurring in the eastern portion of the study area where densities were lower. This correlation complicated separating spatial abundances from temporal variation in behavior and catchability.

The observed directional orientation of yellowtail was behavior dependent (Figure 7). There was no obvious directional orientation of fish that were buried or resting on the substrate. However, swimming fish were highly directional with 84.6% of fish (54 out of 64 individuals) oriented toward the vehicle (negative Y orientation vector).

Fleeing fish swam a mean distance of 0.65m (range = 0.02 - 1.56m) between where they were resting on the bottom and where they were observed (Figure 8). 29% of fish were captured in the same image as their starting point and another 31% were in the image immediately adjacent to their starting point while only two fish were observed >4 images away from their starting point.

Discussion

Results from the *in situ* observation of yellowtail avoidance behavior may be informative both for assessing the efficiency of HabCam and explaining diel variations in the efficiency for other mobile gear types (trawls and dredges, Jacobson 2014). In the case of the HabCam vehicle, yellowtail seem to rely more on camouflage and are less likely to actively flee the gear at night than they are during the day.

Conceptually, the efficiency of an imaging system similar to HabCam may be less than one for multiple reasons including:

1. The fish may be actively swimming in the water column above the altitude of the vehicle and, therefore, not available for sampling.
2. Image analysts may fail to observe a fish in an image due to effective camouflaging or turbid waters.
3. Fish may actively flee the equipment and effectively move themselves out of the imaging track.

Quantifying each of these error rates is complicated by the fact that we have no data on the fish that were missed, only on the ones that were observed.

This study does not contribute to an understanding of availability to the gear but it can start to elucidate issues with observer error and gear avoidance. While partially buried fish are marginally more difficult to discern, they are still readily identified in most clear images and image annotators have been instructed to discard any image where the image quality is poor to further minimize observer errors. The degree to which Yellowtail bury themselves varies but they necessarily leave their head and operculum uncovered for respiration and the caudal fin is usually exposed. Burying behavior was only observed during the night time and thus, observer error may be higher for images captured during the night than during the day. However, given that partially buried fish account for only 8% of the observed fish in the survey, we do not feel that a large portion of the population was missed due to observer error.

This study can also contribute to our understanding of the magnitude of the error in efficiency due to gear avoidance. As with burial, flight behavior also shows a strong diel pattern but is confined to the daytime. Thus, we can similarly assume that gear avoidance error is constrained to daylight hours. Because the probability that a fish successfully avoids the gear increases with flight distance, we can assume that the distribution of flight distances recorded in this study is biased low. However, we point out that the mean recorded flight distance (65cm) is only slightly larger than half the width of the average image track (58cm). Thus, a large portion of fish fleeing off the track should still be partially visible in images, though possibly not counted as “present” in the image. It may be possible to get crude estimates of gear avoidance by modeling the yellowtail behavior based on our collected data but it would require assumptions on preferences in directionality across the survey track vs. along the survey track, where our data is lacking.

The estimation of both observer error and gear avoidance were impeded by the observed spatial gradients in density and the spatiotemporal correlation. These issues could be partially addressed by a well designed and targeted survey of a location with a high density of yellowtail that is repeatedly sampled, varying time of day, current regimes (tide cycles), vehicle altitudes, and other relevant parameters. The addition of a forward-facing camera to the vehicle would also help quantify gear avoidance rates.

Finally, we note that it should be possible to extract burst swimming speeds for yellowtail from this or a similar image set. Within this image set, there are 12 cases where the same flounder appear in sequential photographs. Because the time lag between the images is known, it would be possible to calculate the distance the fish moved between the frames to get a swimming speed. Such data may also be useful for understanding the efficiency of other gears (i.e. limits of herding effects for trawls).

Literature Cited

Adams P, Butler J, Baxter C, Laidig T, Dahlin K, Wakefield W. (1995) Population estimates of Pacific coast groundfishes from video transects and swept-area trawls. Fish. Bull. 93:446-455.

Gunderson D. (1993) Surveys of Fisheries Resources. John Wiley & Sons Inc. New York 248pp.

Jacobson, L. (2014) Prior for Bigelow fall/spring survey catchability and swept area biomass (+ emp q bounds based on diel effects) . TRAC working paper.

Lauth R, Ianelli J, Wakefield W. (2004a) Estimating the size selectivity and catching efficiency of a survey bottom trawl for thornyheads, *Sebastolobus* spp., using a towed video camera sled. Fish. Res. 70:27-37.

Lauth R, Wakefield W, Smith K, (2004b) Estimating the density of thornyheads, *Sebastolobus* spp., using a towed video camera sled. Fish. Res. 70:39-48

Somerton D, Ianelli J, Walsh S, Smith S, Godø O, Ramm D. (1999) Incorporating experimentally derived estimates of survey trawl efficiency into the stock assessment process: a discussion. ICES J. Mar. Sci 56:299-302

Trenkel V, Lorance P, Mahévas S. (2004) Do visual transects provide true population density estimates for deepwater fish? ICES J. Mar. Sci. 61:1050-1056

Uzmann J, Cooper R, Theroux R, Wigley R. (1977) Synoptic comparison of three sampling techniques for estimating abundance and distribution of selected megafauna: submersible vs. camera sled vs. otter trawl. Mar. Fish. Rev. 39:12-19.

Hour	Buried	Surface	Swimming	Fleeing
0		2		
1	8	7		
2		2		
3				
4		8		
5		2		
6		7		
7		6	1	2
8		7	1	9
9		18		5
10		14	1	10
11		3		1
12		17	1	5
13		13		7
14		12		2
15		9		2
16		14	1	8
17		7		4
18		11		2
19	1	2		
20		4		2
21	5	8		
22	6	4		
23	2	10		

Table 1. Number of yellowtail in each size behavior category by hour of the day. Zero abundances were left blank for readability.

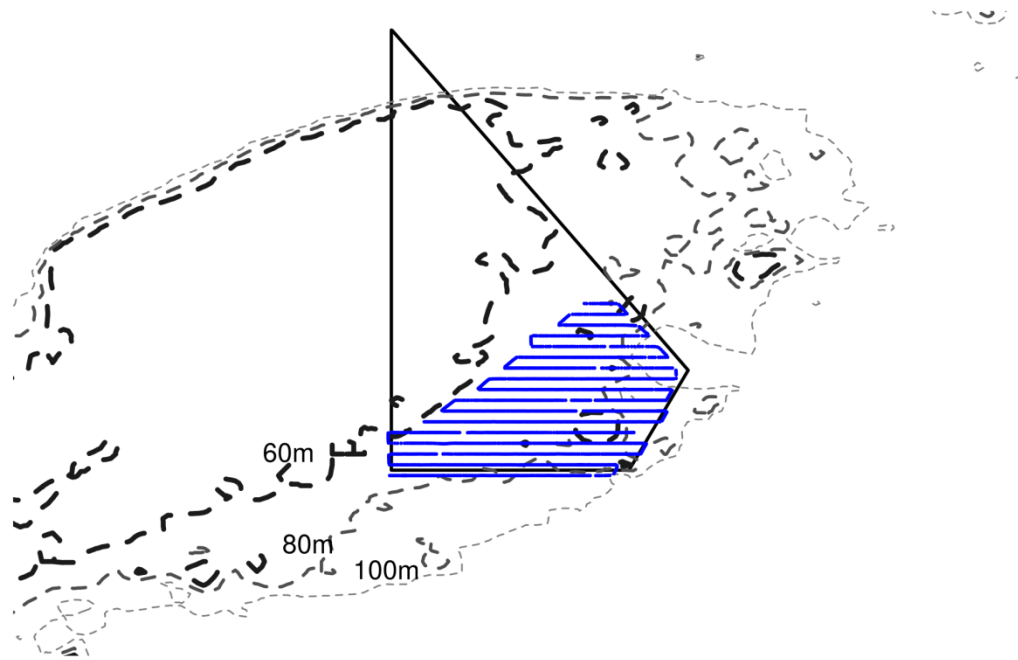


Figure 1. Map of the 2010 HabCam RSA survey area in Closed Area 2 South, Georges Bank.

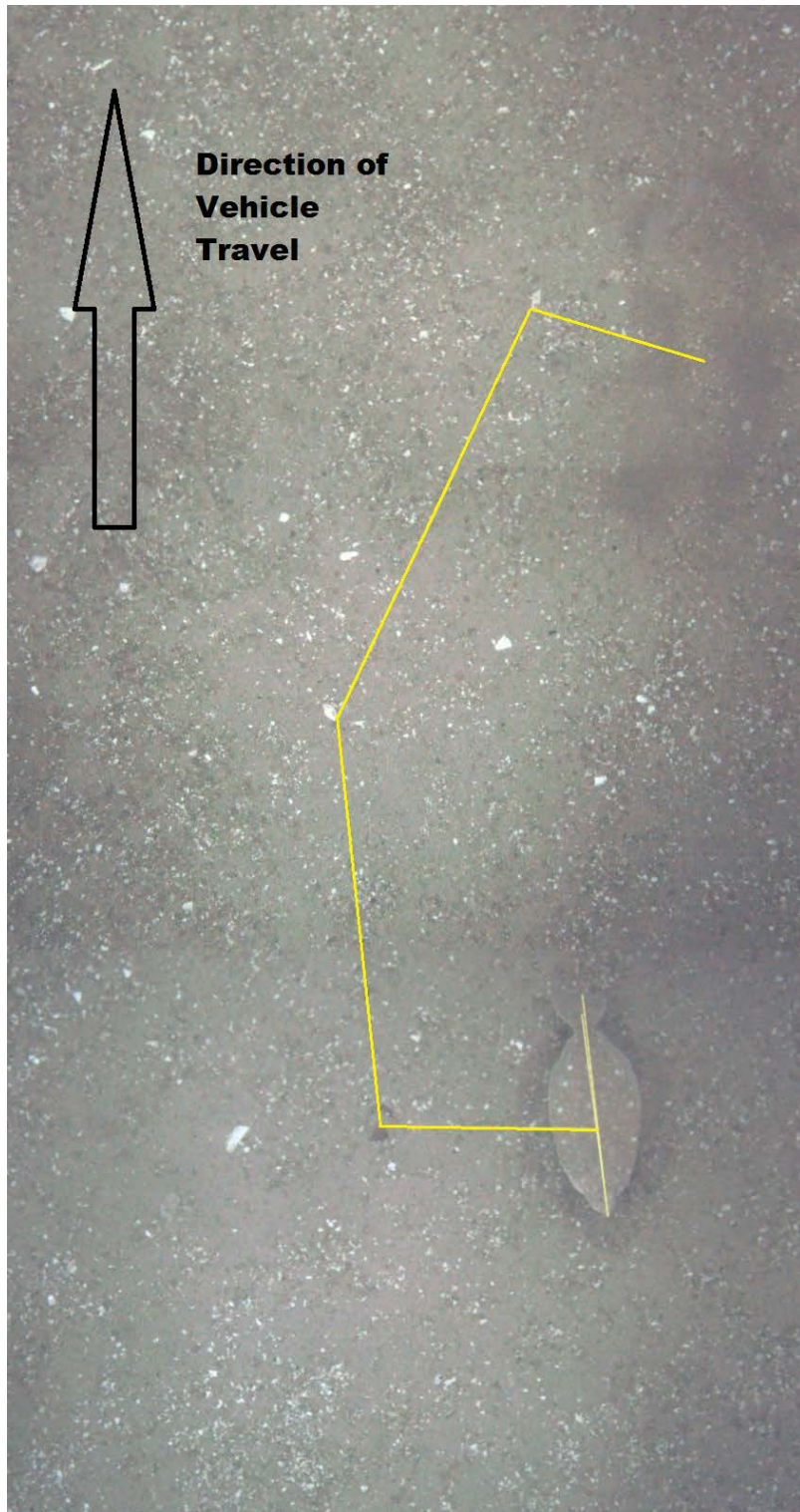


Figure 2. Mosaicked image of a Yellowtail tracked across four images. Yellow lines indicate the line segments summed to calculate the net displacement between the fish and sediment cloud. The longitudinal line on the fish was used to record the orientation of the fish.

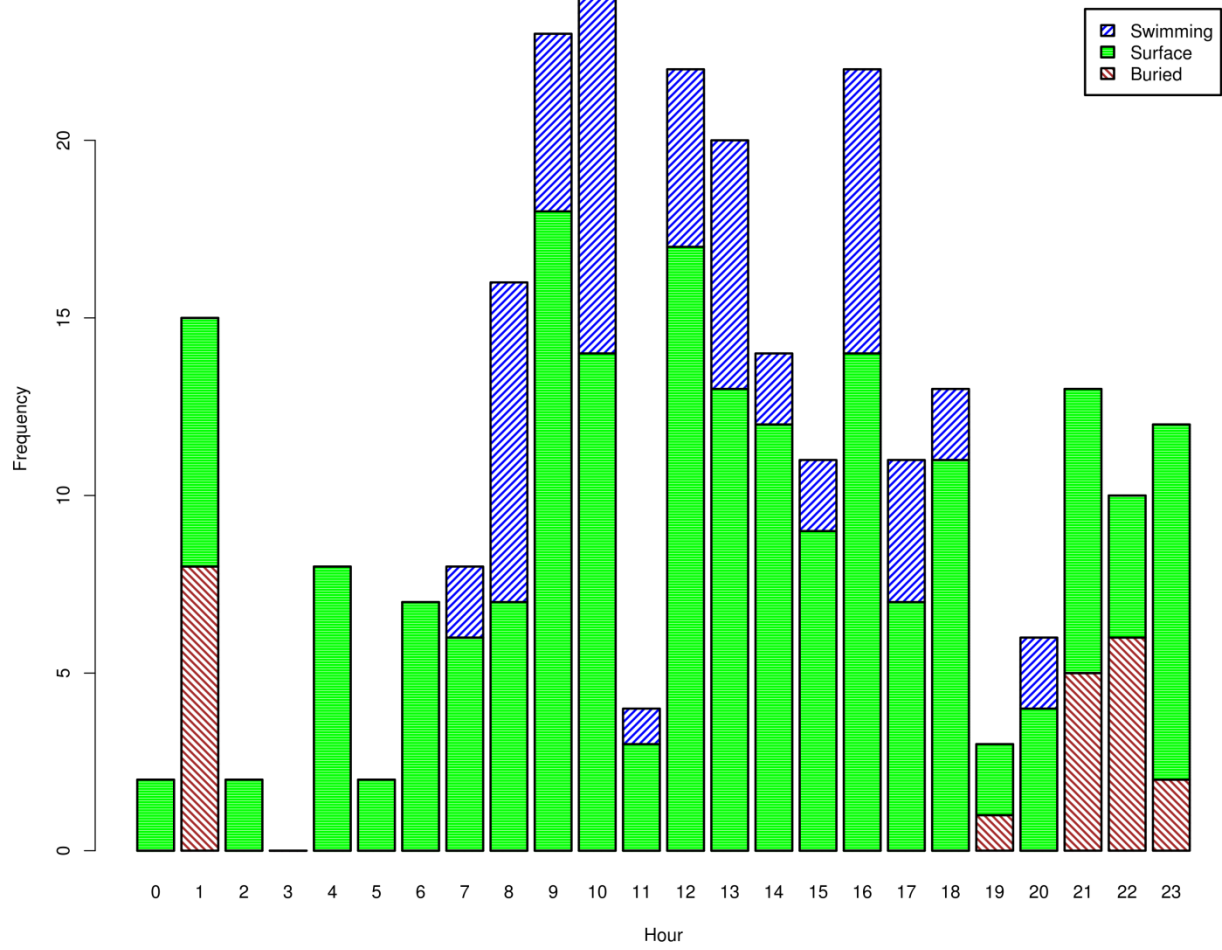


Figure 3. Observed behavior of yellowtail flounder by hour over a diel cycle.

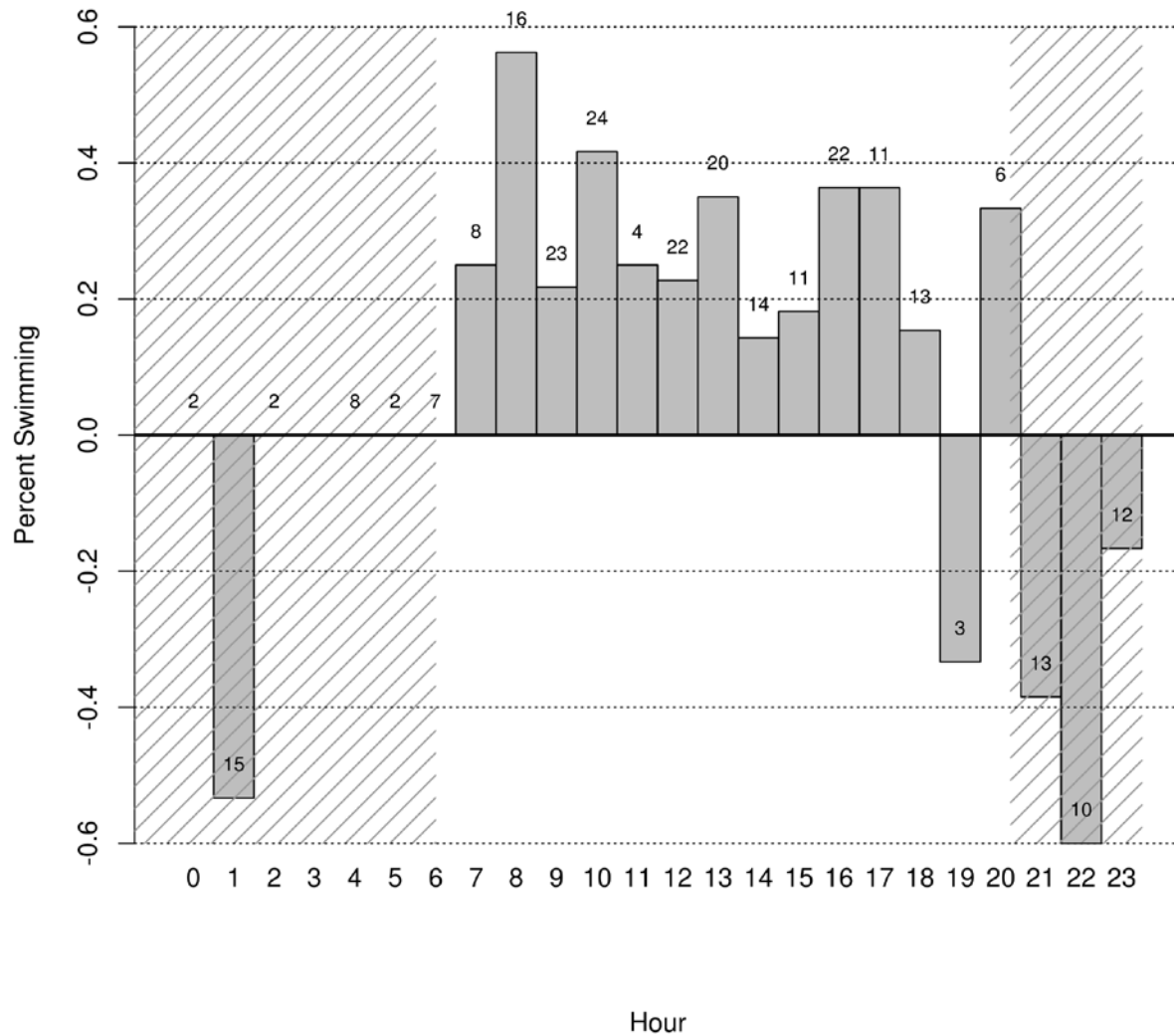


Figure 4. Hourly percent of yellowtail that were observed to be swimming (positive values) or buried (negative values). Superimposed numbers are total sample sizes for the hour.

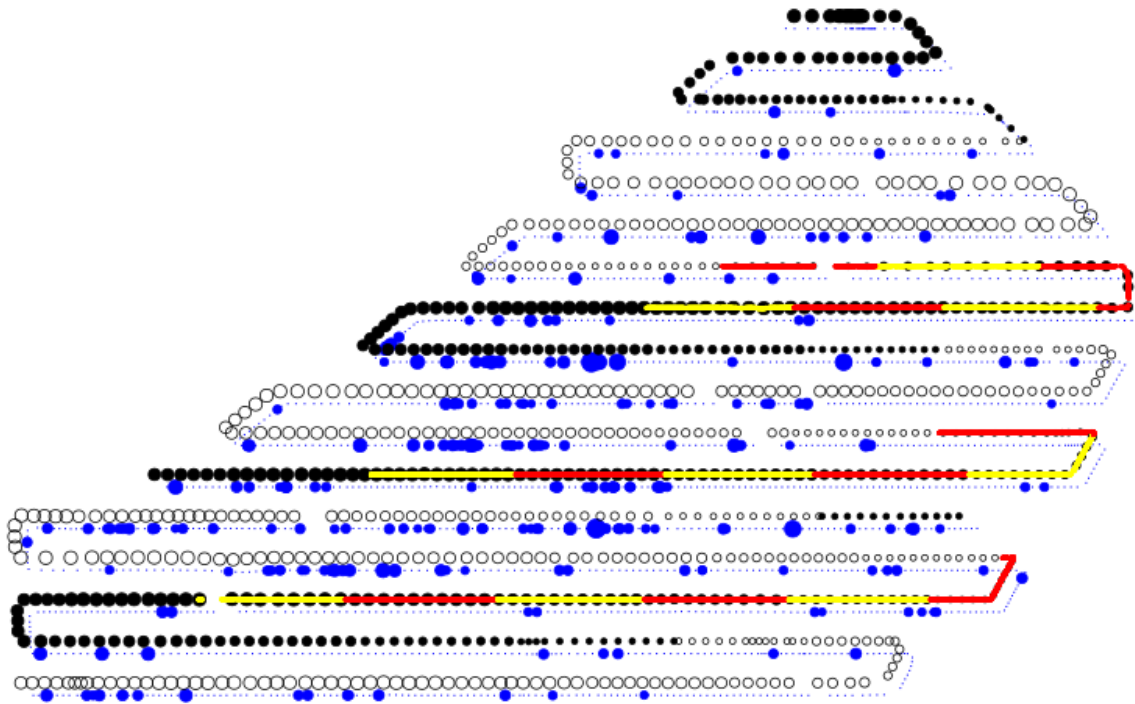


Figure 5. Location of observed yellowtails in 2010 RSA survey. The thin, dotted blue line represents the survey track with larger blue dots representing positive identifications of yellowtail flounder. The second track line, shifted above the survey line indicates the time of day with large, open circles indicating mid-day while large shaded circles indicate late night. The alternating yellow and red segments indicate the hours between 11pm and 5am, approximately left to right.

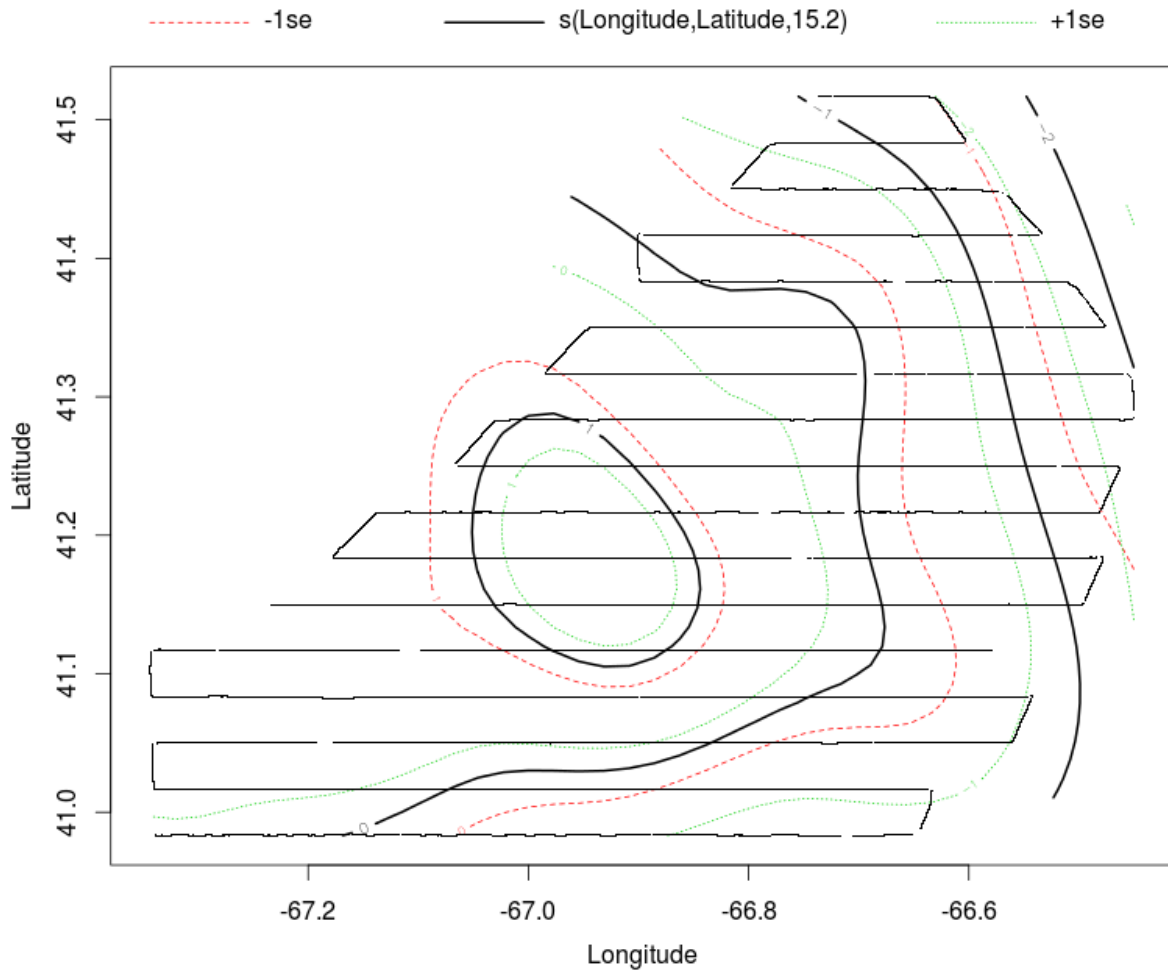


Figure 6. Results from a spatial General Additive Model of yellowtail abundance (Abundance \sim s(Longitude, Latitude)). Highest densities are in the enclosed circle.

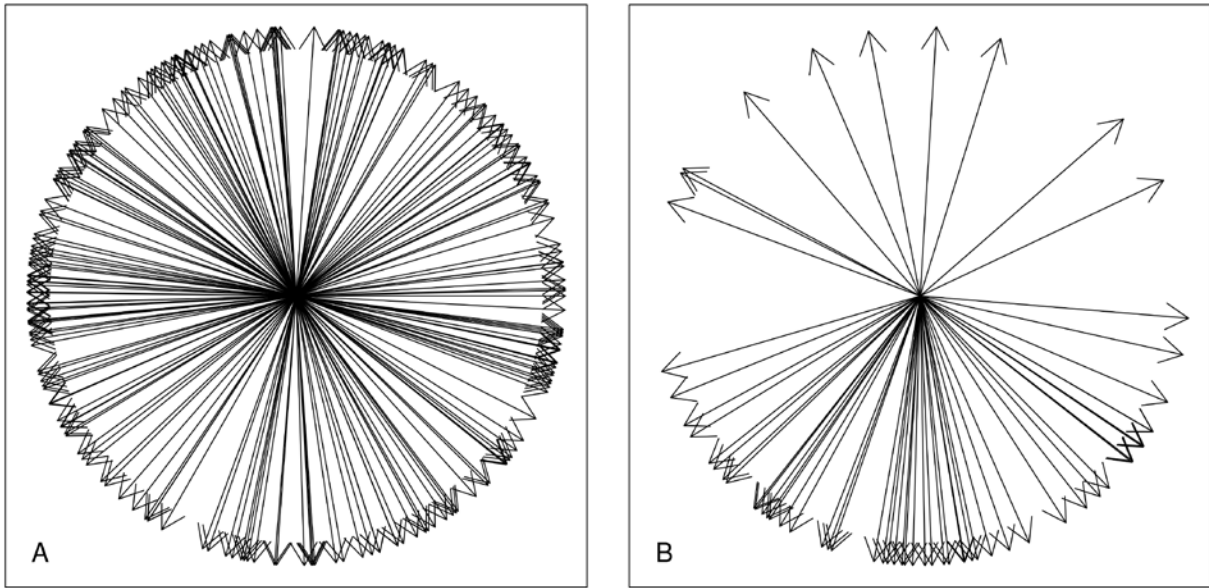


Figure 7. Body orientation of yellowtail flounder that are (A) buried or resting on the substrate and (B) actively swimming relative to the vehicle.

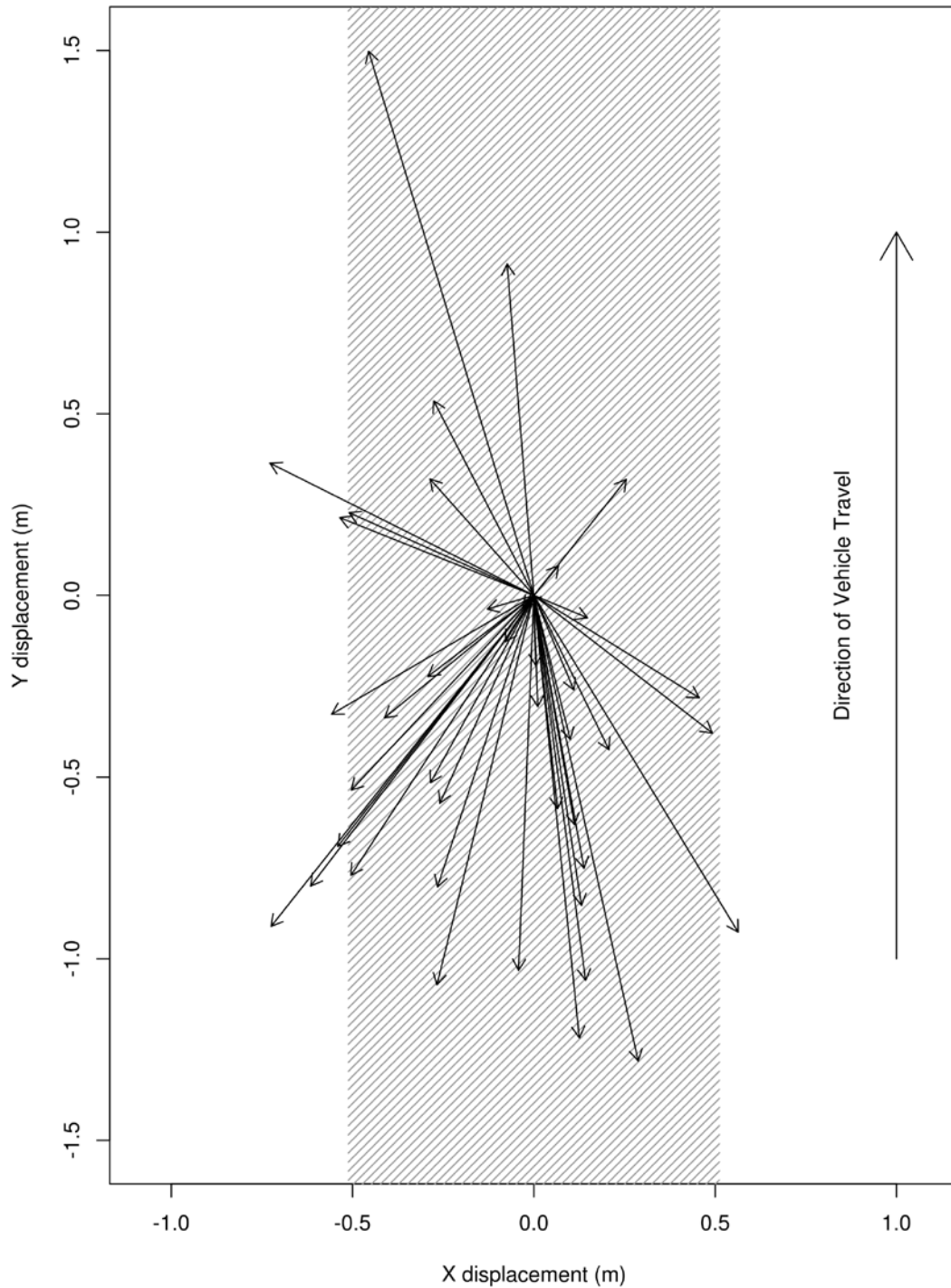


Figure 8. Vectors of net displacement between observed locations of flounder and the cloud of sediment where they were resting. The shaded band indicates the width of a typical image track.